

## Application of artificial intelligence techniques in the estimation of Young's modulus by conventional well logs

Shahoo Maleki<sup>1</sup> , Hamid Reza Ramazi<sup>\*1</sup> , Mohammadjavad Ameri Shahrabi<sup>2</sup>

1-Faculty of Mining Engineering, Amirkabir University of Technology (Tehran Polytechnic), Tehran, Iran

2- Faculty of Petroleum Engineering, Amirkabir University of Technology (Tehran Polytechnic), Tehran, Iran

Received: 10 March 2023; Revised: 29 June 2023; Accepted 23 November 2023

### Abstract

Having information about Young's modulus is extremely essential for characterization of the hydrocarbon reservoirs. This property can be conventionally determined by core sample data analysis in laboratory that is time-consuming, critically expensive and discontinuous. Therefore, many researchers have always been looking for suitable methods to estimate Young's modulus with acceptable accuracy. The current research aims to create an advanced, precise model for estimating Young's modulus by utilizing back-propagation neural network (BPNN), support vector regression (SVR), and gene expression programming (GEP) methods based on the conventional well logs data. Thus, after determination of dynamic Young's modulus, some empirical correlations are proposed for estimation of static Young's modulus. The results demonstrate that the Jambunathan equation is more appropriate than other empirical models. Finally, artificial intelligence (AI) techniques were run, and their results indicated that all techniques (BPNN (R=0.999), SVR (R=0.997) and GEP (R=0.996)) deliver highly accurate values of static Young's modulus. Comparing these results shows that the BPNN technique is relatively more precise than other ones. Although, in this research, the GEP technique was not more accurate than BPNN and SVM techniques, it provides a new nonlinear equation that can be used for estimating Young's modulus in other similar fields. As a new finding, it was found that a simultaneous combination of the Jambunathan equation and BPNN technique delivers highly accurate results. Hence, it can be applied to slim down the cost of exploratory operations for determination of the Young's modulus of limestone rocks.

**Keywords:** Gene expression programming, Young's modulus, well logs data, Back-propagation neural network, Support vector machine, core sample data.

### 1. Introduction

In earth science engineering, Young's modulus is a criterion to evaluate the rock strength. Moreover, it can be applied for estimation of different geological and geomechanical characteristics of the underground reservoirs. Such characteristics include the in situ stress (Lai et al. 2022), and poroelastic properties (Knez and Zamani 2021). Young's modulus is determined through experimental tests on the rock samples, or acoustic waves in the oil/gas fields. Laboratory analysis to determine Young's modulus is uniaxial and triaxial compressive strength or pulse transmission techniques (Chang et al. 2006; Watanabe et al. 2007; Ameen et al. 2009; Zoback 2010) that are time-consuming, expensive, and discontinuous (Khaksar et al. 2009; Abdulraheem 2009; Elkatatny et al. 2019). By contrast, fields data for estimating Young's modulus are well logs and seismic waves (Zoback 2010; Maleki et al. 2014a, b) which are inexpensive and continuous over the whole well interval or reservoir. Therefore, the geophysical methods provide the researchers with a larger amount of recorded data in comparison to the conventional exploration techniques such as vertical boreholes and shallow trenches (Mostafaei and Ramazi 2018).

Generally, the dynamic Young's modulus ( $E_{dyn}$ )

achieved through estimating wave velocities lies in a wide range; hence the Young's modulus extracted from well logs or seismic data are converted to the static Young's modulus ( $E_s$ ) by utilizing calibration (Zoback et al. 2010; Resouli et al. 2001; Maleki et al. 2014a, b). To address this issue, several empirical equations were already proposed in the last decades (King 1983; Eissa and Kazi 1988; Bradford et al. 1998; Wang 2017; Fjar 2008; Jambunathan 2008; Canady 2011). Usually, such empirical equations were provided for a specific formation with certain geological and tectonic conditions. Consequently, to apply those equations in similar cases all of these parameters and conditions must be considered. Yet, in many cases, such empirical equations show inaccuracy in estimation of Young's modulus. Consequently, their application, in the identical cases, does not seem logical.

Considering the aforesaid problems, many researchers have always been looking for ways that are appropriate to replace the empirical equations with high-accuracy estimation methods (Mostafaei and Ramazi 2015). One of those methods, that has attracted the attention of many researchers, is artificial intelligence (AI) tool (Elkatatny et al. 2019; Mahmoud et al. 2019; Gowida et al. 2019; Mostafaei et al. 2022). The AI techniques can predict different unknown variables with remarkable precision. For example; BPNN, ANN, SVM and, ANFIS were

\*Corresponding author.

E-mail address (es): [ramazi@aut.ac.ir](mailto:ramazi@aut.ac.ir)

utilized for estimating Young's modulus using the well logs data. Those researches showed that the ANN technique is the most appropriate method for Young's modulus estimation in comparison with the SVM and ANFIS. More artificial intelligence techniques are boxed which cannot be applied to other similar cases. Therefore, alteration and replacement of these techniques, which are not efficient with other AI techniques, may mitigate the potential problems and shortcomings.

In this research, the conventional well logs data relevant to an Iranian carbonate reservoir oil field has been used for Young's modulus estimation by BPNN, SVR, and GEP techniques. Eventually, a new equation from the GEP technique has been presented that can be used to other wells in this field as well as in other fields in which the geological and conditions are similar.

## 2. Samples and methods

### 2.1. Geological and geomechanical description

In this study, the data of an onshore oil reservoir located in the Khuzestan province, Abadan plain, near the Iran-Iraq frontier was used. The Abadan plain is located within the Mesopotamian foredeep basin in the southwest of Zagros foreland. Prior to the final collision, the oceanic domain between the continents had been under convergence at least since the late Eocene time. The Zagros foreland basin comprises the syn- and post-Zagros collision succession (upper Miocene to Holocene), which, together with the deeper units (i.e. post Permian succession), has been deformed by the subsequent folding and thrusting events. The Zagros foredeep basin area includes many super giant oil and gas fields (Fig 1). The current oil field is around 23 kilometers in length, and 9 kilometers in width. Moreover, the trend of the structure is a special case to the belt of the foothill fold of southwestern Iran, striking

NW-SE direction. In addition, regional unconformities were present at the top of Dariyan, Sarvak, Gurpi, and Jahrum formations which show the effect of epirogenic movements. Above the Tarbour Member (inside the Gurpi Formation), there is no structure closure, and it seems that this area was tilted to the NE due to Zagros orogeny. Since the hydrocarbon reservoir is located inside the Fahliyan Formation, it is one of the crucially important constructors which should be checked. This formation is superbly represented within the Zagros Mountains (James and Wynd, 1956; Karimiazar et al. 2023). Fahliyan formation was formed simultaneously to the intrashelf basin of the Garau formation. The prevalent oil field must be dependent on an articulate carbonate ramp intricate, somewhat governed by the regional tectonics state, and by the sea surface plate changes. The presence of limestone and shales in the deep surroundings indicates that this region belongs to the identical intrashelf basin. In the last Tithonian and the primary Berriasian, the sedimentation of those rocks depends on the remarkable sea level rise (Sadooni, 1993; Dehghan and Yazdi 2023). The little depth water sequences of Fahliyan formation and analogous of northern Persian Gulf underlay the shale and bioclastic limestone of the Ratawi formation. Well logs data, which have been chosen in the current research, is relevant to a borehole drilled vertically through a carbonate reservoir. The digitized well logs data comprises the Density log (RHOB), Shear wave velocity log (Vs), Caliper log (CAL), True formation Resistivity log (RT), Compressional wave velocity log (Vp), Total porosity log (PIGT), Poisson's Ratio log (PR), and Gamma ray log (GR). The plots pertinent to these logs have been shown in Fig 2. Finally, the static Young's modulus was determined by computing the slope of the stress-strain curves (Table 1).



Fig 1. The map of different oil fields in Zagros foredeep basin.

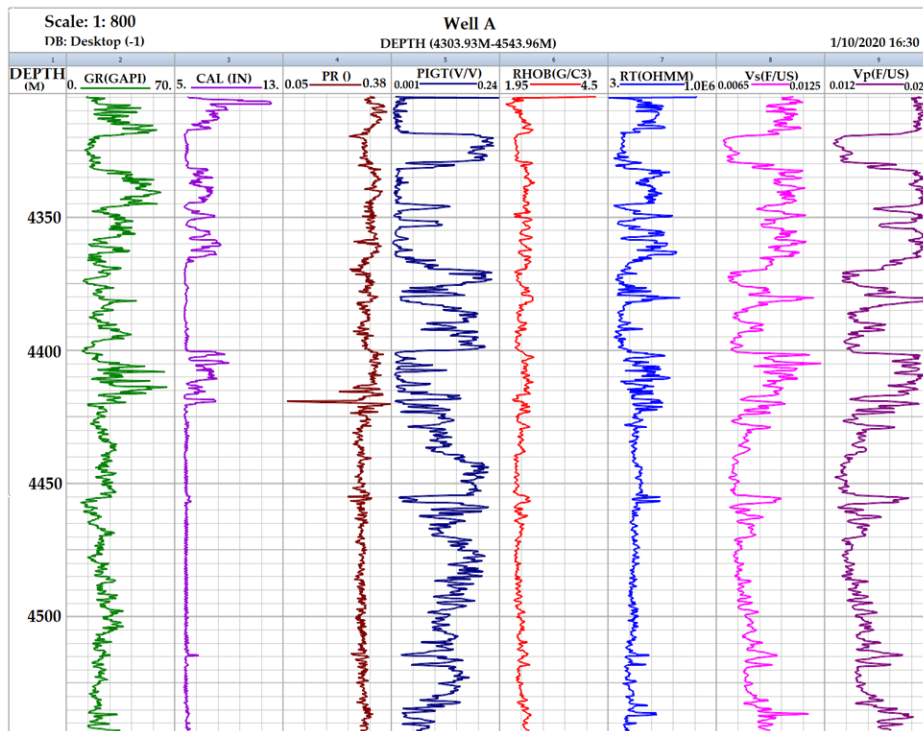


Fig 2. Well logs utilized for Young’s modulus estimation in this research.

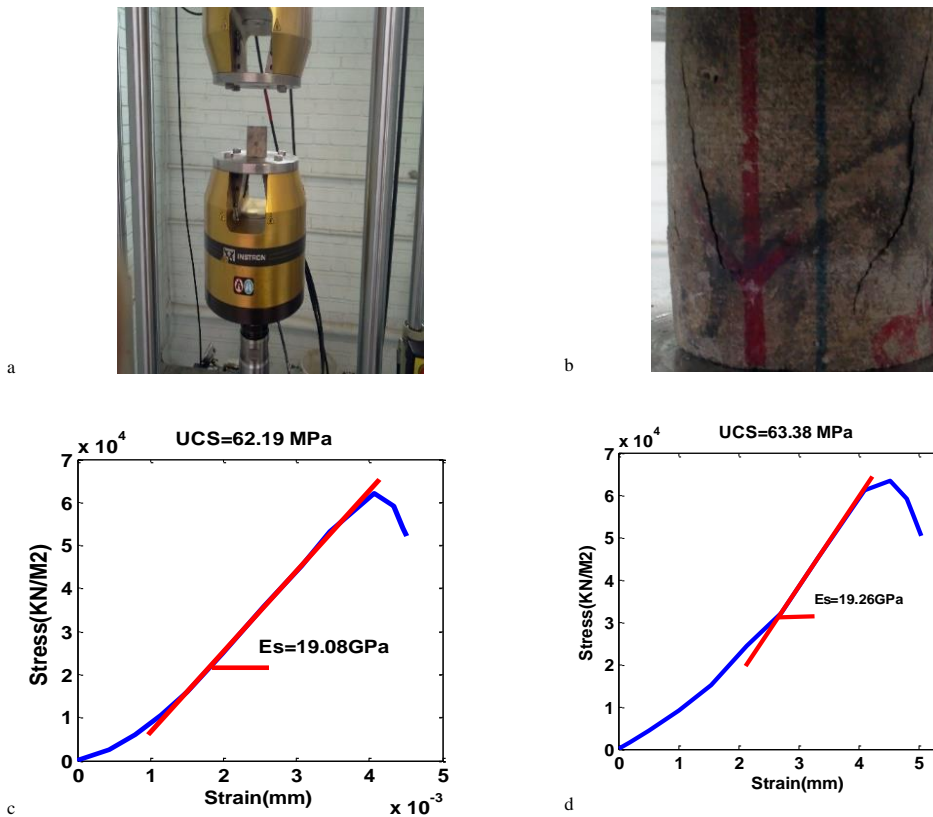


Fig 3. Schematics of core sample analysis by the UCS tester in laboratory and its results (two samples): (a) Specimen prior to the UCS test (b) Specimen after the UCS test (c) Stress and strain curve for core sample no. 2 (d) Stress-strain curve for core sample no. 3.

Table 1. The different characteristics of the four core samples.

Sample code	Depth (m)	UCS (MPa)	Es (GPa)
No. 1	4321	80.93	9.7
No. 2	4328	62.19	19.08
No. 3	4426	63.38	19.26
No. 4	4440	79.41	19.86

## 2.2. Empirical equations

S-wave and P-wave velocity logs were utilized estimate the dynamic Young's modulus ( $E_{dyn}$ ). To do this, Equation 1 was applied (Zoback 2010; Maleki et al. 2014; Knez and Zamani 2021):

$$E_{dyn} = \rho V_S^2 \frac{3V_P^2 - 4V_S^2}{V_P^2 - V_S^2} \quad (1)$$

Where  $E_{dyn}$  represents the dynamic Young's modulus, and  $\rho$  indicates the bulk density ( $\text{gr/cm}^3$ ). Moreover,  $V_S$  (km/s) and  $V_P$  (km/s) represents the shear wave and compressional wave speeds, respectively.

In general,  $E_{dyn}$  is always different from its real value denominated as  $E_s$ . The  $E_{dyn}$  is commonly 1.5-3 times higher than the  $E_s$  (Larsen et al. 2000). To avoid this issue, various empirical equations were proposed by different geomechanics and geophysics researchers. Those empirical equations have been offered to specific reservoir formations with particular conditions. The reservoir rock type in the study area is limestone; hence the empirical equations related to the  $E_s$  estimation for limestone formations were chosen. Some of those empirical equations are elaborated in the following section.

### 2.2.1. Eissa and Kazi equation

The Eissa and Kazi equation is one of the most applicable empirical equations for  $E_s$  estimation in limestone formations (Eissa and Kazi 1988). They utilized 714 Young's moduli and proposed the following equation:

$$E_S = 0.77E_d + 0.02 \quad (2)$$

### 2.2.2. Fjar et al equation

Fjar et al, (2008) offered the following relation for limestone rocks as:

$$E_S = 0.018E_d^2 + 0.422E_d \quad (3)$$

### 2.2.3. Wang equation

Wang (2017) offered the underlying empirical equation for limestone rocks:

$$E_S = 1.153E_d - 15.197 \quad (4)$$

### 2.2.4. Venkataraman Jambunathan equation

Jambunathan, (2008) proposed the underlying empirical correlation for limestone rocks:

$$E_S = 0.84E_d + 0.7 \quad (5)$$

## 2.3. AI methods

### 2.3.1. BPNN algorithm

The ANNs mimic the biological neural units to establish a mathematical pattern. There are many types of ANN, but one of their best is the BPNN algorithm. BPNN has been vastly utilized by different investigators (Maleki et al. 2014a). There are different researches who have confirmed the capability of BPNN algorithm (Plett 2003; Maleki et al. 2014a). BPNN technique has a remarkable capability to solve the different engineering problems. As an illustration, Jin and Gupta investigated the stability of dynamic back propagation training approach using the Lyapunov technique (Jin and Gupta 1999). Such a network is commonly trained with both input and output parameters. The algorithm strives to match the output variables with the suitable values in the training process. To train the model, firstly, some random weights are specified. Afterwards, the output parameters are computed, and the corresponding error is calculated. Then, the operation continues until the calculated error reduces to its minimum value. In this way, the weights are updated. To stop the operation, the average error of epoch is commonly utilized.

### 2.3.2. SVR algorithm

SVM is also known as support vector regression (SVR). SVR finds an approximation function for the output variable (Cristianini and Shawe-Taylor 2000; Maleki et al. 2014a). The SVR utilizes a number of training samples, known as support vectors, to find the approximation function. Moreover, this algorithm deploys a particular loss function, known as  $\mathcal{E}$ -insensitive, to generate an accurate sparseness feature. This algorithm was established using the regression approach along with the inner product of two vectors in the Hilbert space. To minimize the risk, the error and complexity of the model are simultaneously controlled. The SVR applies this concept for improvement of its generalization capability (Martinez-Ramon and Cristodoulou 2005). On the other hand, the data points are always mapped into the feature space to increase the generalization. This task is performed by the kernel function (Steinwart and Christmann 2008; Maleki et al. 2014a).

If an appropriate kernel function is selected, the data can be then separated in the feature space while the former input space remains non-linear. Therefore, when the hyper plane cannot separate the data, an accurate Kernel function will separate it (Scholkopf et al, 1998; Maleki et al, 2014a). It should be noted that the SVR is capable of performing any non-linear regression solution (Sanchez 2003; Maleki et al. 2014a).

### 2.3.3. GEP algorithm

Initially, the GEP method was developed as an applicable technique for making computer programs and codes (Ferreira 2001). These models and programs include complicated tree structures which learn and confirm through modifying the composition, scales and forms, exactly similar to a living organism. This algorithm is almost similar to the genetic programming (GP) and genetic algorithm (GA) methods encoded in simple linear chromosomes of constant length (Mithcell 1996).

The basic discrepancy between the GAs, GP, and GEP approaches is stemmed from the essence of the individuals. Regarding the GP algorithm, the individuals represents non-linear beings which have diverse dimensions and shapes. Concerning the Gas, it can be stated that the individuals represents linear strings with constant length.

When it comes to the individuals in a GEP algorithm, they represent linear strings with constant length (the genome or chromosomes) that are subsequently referred as non-linear existents with inconsistent dimensions and shapes. To solve a problem by GEP algorithm, like GP method, generally five parameters are needed. Those parameters include the terminal set, the function set, fitness function to evaluate the fitness formulas, controlling variables, and stop criterion (Ferreire 2001). In the GEP algorithm, firstly, the initial population of chromosomes are generated, and then, the generated chromosomes function as expression trees. Afterwards, for every individual, the fitness function is assessed, and the best individuals are chosen. The new individuals are then subjected to a similar process until the stop criterion is satisfied (Ferreira 2001). Figure 4 depicts the schematic GEP approach flowchart.

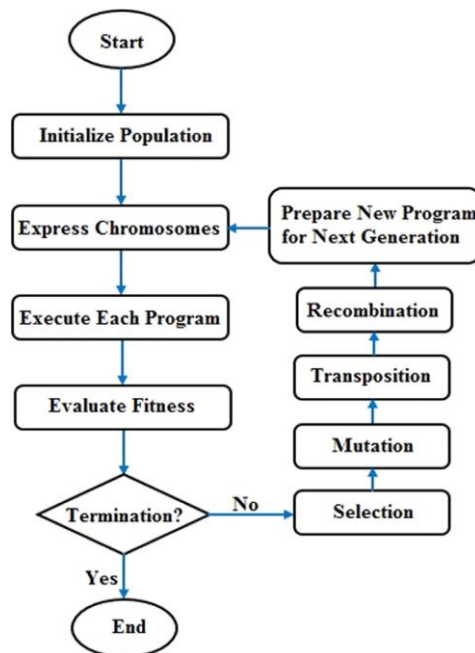


Fig 4. GEP algorithm flowchart (Faradonbeh et al. 2016).

Consequently, in general, it can be said that the GEP algorithm uses the linear genomes as a genetic basis, and operators such as mutation, crossover, recombination, inversion, and transposition. The genome expressed by chromosomes and each chromosome is composed of genes translated to ETs for solving a complex problem. For detailed information about the GEP algorithm see Ferreira book (Ferreira 2006).

## 3. Results and discussion

### 3.1. Empirical equations

As already mentioned, various empirical relations have previously correlated the  $E_s$  with the  $E_{dyn}$ . In this research, the  $E_s$  values were estimated from Equations 2, 3, 4, and 5, and then, they were calibrated with the  $E_s$  values of

specimens whose curves have been shown in Fig 5. Moreover, the empirical equation from the  $E_s$  obtained from the core sample data (See Table 1) was used to estimate the  $E_s$  using the  $E_{dyn}$  (Eq. 6) which its result has been shown in Fig 5. Note that the  $E_s$  values of the core specimens have been illustrated as blue solid circles in Fig 5.

$$E_s = 2.14E_d - 46.96 \quad (6)$$

The comparison of the empirical equations results with the real data (Fig. 5) shows that the Jambunathan equation in (E V. Jambunathan) is more suitable than other equations to estimate the  $E_s$ . The equation of this study (Eq. 6), that has been used to determine the  $E_s$  values, is appropriate but it is not more accurate than

Jambunathan equation because the number of core samples data is low (four core samples). Therefore, the  $E_s$  estimated by Jambunathan equation (Eq. 5) has been used in the current research.

**3.2. AI algorithms**

Before selecting the artificial intelligence techniques, the best well logs data must be prepared for  $E_s$  estimation. To do this, the principal component analysis (PCA) was applied in the current research. The corresponding results have been tabulated in Table 2.

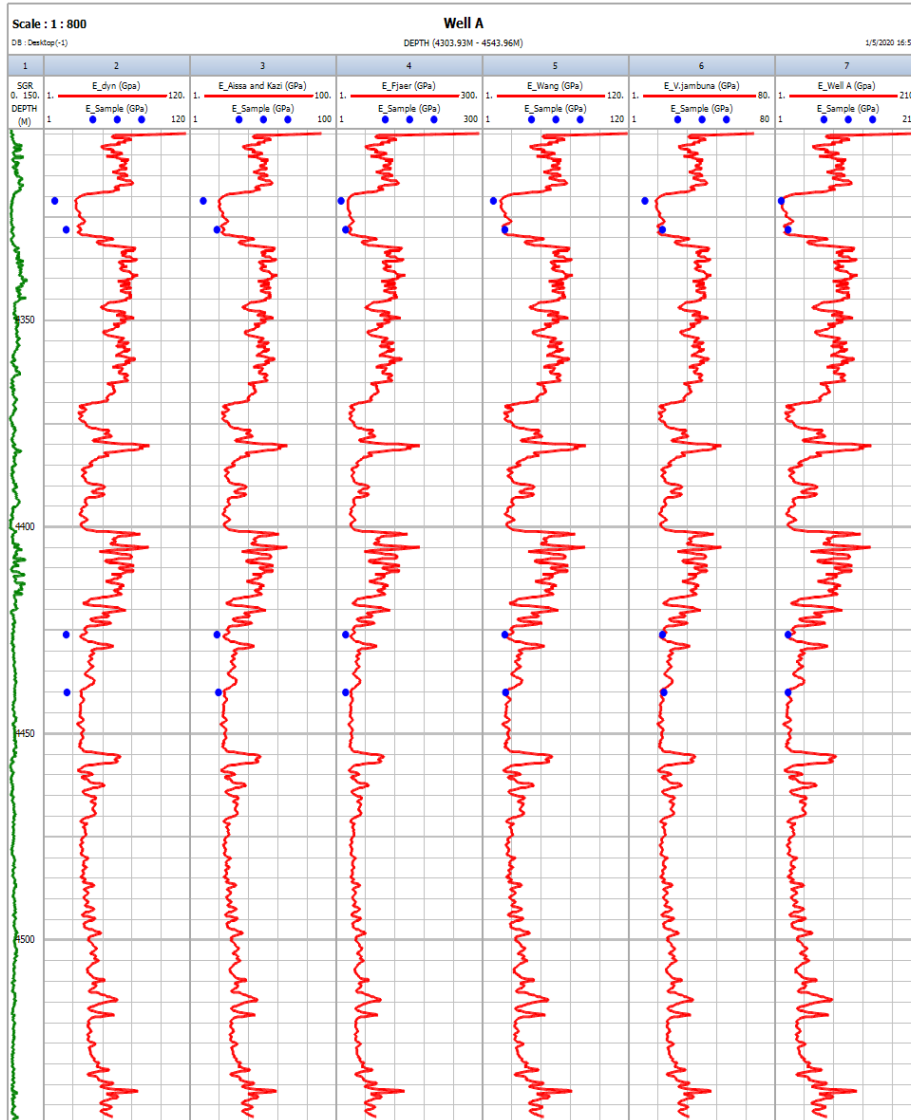


Fig 5. The  $E_s$  estimation curves (red color lines) through utilizing empirical equations (Equations 2-6) and real Young's modulus data of the core specimens (blue points).

Table 2. Correlation matrix between well logs data and static Young's Modulus.

	$E_s$	PR	RHOB	GR	RT	CAL	Vp	Vs	PIGT	
Pearson Correlation	$E_s$	1.000								
	PR	.532	1.000							
	RHOB	.710	.316	1.000						
	GR	.460	.248	.289	1.000					
	RT	.244	.085	.426	-.015	1.000				
	CAL	.614	.431	.092	.289	.085	1.000			
	Vp	.963	.584	.626	.503	.140	.651	1.000		
	Vs	.984	.506	.592	.445	.158	.671	.955	1.000	
	PIGT	-.890	-.467	-.646	-.459	-.127	-.642	-.904	-.885	1.000

According to Table 2, it can be concluded that the PR, RHOB, CAL,  $V_p$ ,  $V_s$  and PIGT logs data have high correlation coefficients with the  $E_s$ . Consequently, these well logs data were imported as input parameters for  $E_s$  estimation.

**3.2.1. The BPNN results**

For  $E_s$  estimation, the most suitable input parameters were obtained from the PCA method (See section 5.2). The dataset consisted of six input parameters (PR, RHOB, CAL,  $V_p$ ,  $V_s$  and PIGT logs), and the output was  $E_s$  log obtained from the Jambunathan equation. These datasets were broken down into the training and testing categories with a ratio of 70% to 30%, respectively. Then, the BPNN algorithm was run in MATLAB software. The optimum network consisted of one input layer including six neurons (each of those is one well log), three layers of sigmoidal function including twelve neurons, and the output layer including only a single neuron (static Young’s modulus). The BPNN algorithm was run with these conditions in a number of 1000 epoch, and then, the best results for  $E_s$  values in well A were calculated. Fig 6 shows the corresponding results.

As it can be seen, the correlation coefficient of BPNN algorithm (left) during the testing process found to be 0.999; hence the BPNN algorithm is a highly reliable, accurate approach for  $E_s$  estimation.

**3.2.2. The SVR results**

In this research, another code was developed in MATLAB multipurpose software to estimate the  $E_s$ . To

do this, the optimum Kernel function along with the optimal values of parameters ( $\lambda$ ,  $\epsilon$  and  $C$ ) were required. If the Kernel function and other parameters are determined correctly, the estimated value of  $E_s$  is predicted very accurately. There are various researches on the best performance Kernel functions that can be used in SVR (Keerthi and Lin 2003; Maleki et al. 2013; Maleki et al. 2014a; Gholami et al. 2014). According to those studies, Gaussian or Radial basis function (RBF) was reported as a potent Kernel function with theoretical simplicity and computational convenience. The mathematical form of the Kernel function can be expressed as:

$$K(x_i, x_j) = e^{-\|x_i - x_j\|^2 / 2\sigma^2} \tag{7}$$

Where  $\sigma$  represents the parameter of Kernel. The amplitude of the Gaussian function or the generalization capability of the SVR algorithm is controlled by this parameter.

It should be noted that as well as the appropriate kernel function, the kernel parameter ( $\sigma$ ), capacity parameter ( $C$ ), regularization parameter ( $\lambda$ ) and insensitive parameter ( $\epsilon$ ) are needed to be optimally selected for SVR. In this study, the optimum  $\sigma$ ,  $C$ ,  $\lambda$  and  $\epsilon$  obtained from the trial and error test approach were as 0.13, 900000, 0.000001 and 0.1, respectively. After running the SVR code with those values, the results were acquired (Fig 7).

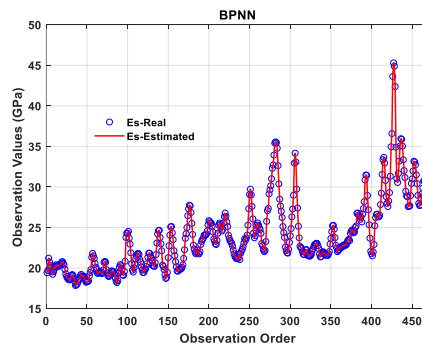
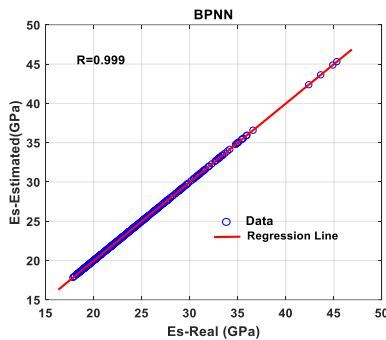


Fig 6. Correlations between the measured and estimated  $E_s$  using BPNN (left), and the estimation performance of the BPNN algorithm (right).

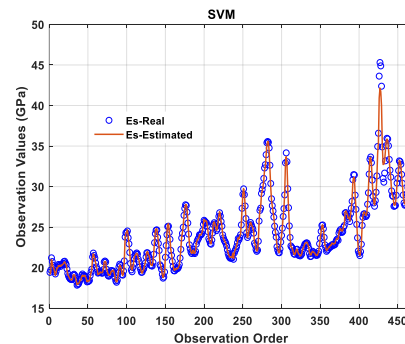
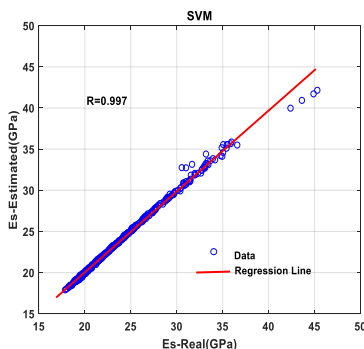


Fig 7. Correlation between the measured and estimated  $E_s$  by SVR (left), and the estimation performance of SVR (right).

The SVR model showed a high correlation coefficient ( $R=0.997$ ) in the testing stage. This matter has been depicted in Fig 7 (left). Furthermore, the estimation performance of the SVR model was high (Fig 7 (right)). Therefore, the SVR algorithm is an accurate approach to estimate the  $E_s$  although its precision is less than BPNN algorithm.

**3.2.3. The GEP results**

In this research, the GEP algorithm by GeneXproTools 5.0 software was utilized for  $E_s$  estimation. The dataset

consisted of six input parameters (PR, RHOB, CAL, VP, VS and PIGT well logs data), and one output parameter ( $E_s$ , Jambunathan). This dataset was broken down into the training and testing datasets with the ratio of 70% to 30%, respectively. After applying the select function set (addition, subtraction, multiplication, division, power and square root) in GeneXproTools software, and performing a thousand runs for GEP algorithm, the best results of those runs were chosen (Fig 8)

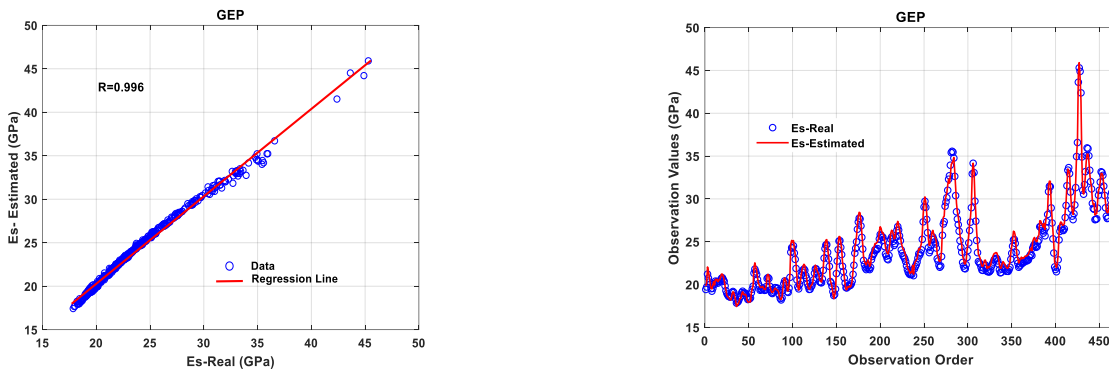


Fig 8. Correlation between the measured and estimated  $E_s$  using GEP (left), and estimation performance of GEP (right).

The GEP model delivered a high correlation coefficient ( $R=0.996$ ) in the testing stage (Fig 8 (left)). In addition, the estimation performance of the GEP model (Fig 8 (right)) is suitable although it's not better than two other models (BPNN and SVR models). The fundamental difference between the GEP method and two other methods (BPNN and SVR algorithms) is that it provides a set of equations which can be used in similar cases for estimating the  $E_s$  values. In the current research, three nonlinear equations were obtained from expressions trees that these equations can be used in other similar oil fields to predict the  $E_s$  values:

$$E_s = [RHOB - (CAL + [CAL - 0.5974])] - \left[ \frac{PR}{V_s \times (RHOB - 0.1288)} \right] \quad (8)$$

$$E_s = 9.43446 - \left[ \frac{V_s^{RHOB}}{7990024547.68315} \right] \left( \frac{9.93199 \times V_s}{RHOB} \right) \quad (9)$$

$$E_s = [RHOB \times (PIGT^{RHOB} + RHOB)] \times [(V_p + PR) \times (CAL + 3.9358)] \quad (10)$$

where  $E_s$  represents the static Young's modulus (GPa), RHOB indicates density ( $gr/cm^3$ ), CAL is caliper (in), PR represents the Poisson's ratio,  $V_s$  indicates S-wave speed ( $ft / \mu s$ ), PIGT manifests the total porosity (V/V), and  $V_p$  shows the P-wave speed ( $ft / \mu s$ ).

**4. Discussion**

To compare the performance of the applied AI algorithms, their root means square error (RMSE) together with the correlation coefficient (R) bars chart have been plotted in Fig 9



Fig 9. Bar-chart of the RMSE (right) and correlation coefficient (left) for estimating of  $E_s$  by BPNN, SVM, and GEP methods.

Fig 9 shows that the best value of correlation coefficient (R) and also the least value of RMSE is related to the BPNN technique. It should be noted that two other techniques are suitable for  $E_s$  estimation although their precision and performances are less than the BPNN technique. Consequently, the BPNN technique is remarkably appropriate for estimating the  $E_s$  values.

## 5. Conclusions

In current research, the static Young's modulus,  $E_s$ , was estimated using the conventional well log data pertinent to an oil field with limestone rocks in the south of Iran. The  $E_s$  was estimated by three AI algorithms including BPNN, SVM, and GEP techniques from conventional well logs data.

From the conducted research, it was concluded that:

1. The BPNN, SVM, and GEP algorithms are potent tools for  $E_s$  from conventional well log data.
2. Correlation coefficient (R) for BPNN technique was equal to 0.999, and hence, it indicates that its accuracy is higher than other two techniques (SVM (R= 0.997) and GEP (R=0.996)).
3. The RMSE of the BPNN technique was equal to 0.000867 that is less than the obtained values for both SVM (RMSE=0.34) and GEP (RMSE=0.56) techniques.
4. The BPNN method is the most appropriate AI technique for  $E_s$  estimation in comparison to the SVM and GEP methods.
5. The GEP method offers three equations based on the conventional well logs (density log, caliper log, Poisson's ratio log, porosity log, P- wave and S- wave velocity logs) for  $E_s$  estimation that can be used in other similar cases.
6. The accuracy and performance of BPNN technique is much better than other two techniques (See, Fig 6, Fig 7, and Fig 8).
7. Empirical equations were calibrated by actual Young's modulus from core sample data. Their results show that the Jambunathan equation is the best one to predict the  $E_s$  through the  $E_{dyn}$ .

The applied AI techniques aid the rock mechanics and petroleum engineers for  $E_s$  estimation based on the conventional well logs. These techniques are extremely inexpensive to determine the  $E_s$  values throughout a certain reservoir that its conventional well logs are available. A novel discovery was that results are extremely accurate when the Jambunathan equation and BPNN approach are used simultaneously. As a result, it can be used to reduce the expense of exploratory activities for figuring out the limestone formations' Young's modulus.

## References

Abdulraheem A, Ahmed M, Vantala A, Parvez T (2009) Prediction of rock mechanical parameters for hydrocarbon reservoirs using different artificial intelligence techniques. In Section Technical Symposium (SPE), Saudi Arabia.

- Ameen MS, Smart BG, Somerville JM, Hamilton S, Naji NA (2009) Predicting rock mechanical properties of carbonates from wireline logs (A case study: Arab-D reservoir, Ghawar field, Saudi Arabia), *Marine and Petroleum Geology* 26(4):430-44.
- Bradford ID, Fuller J, Thompson PJ, Walsgrove TR (1998) Benefits of assessing the solids production risk in a North Sea reservoir using elastoplastic modelling. International Society for Rock Mechanics and Rock Engineering.
- Canady WJ (2011) A method for full-range Young's modulus correction. In unconventional gas conference and exhibition, North American.
- Chang C, Zoback MD, Khaksar A (2006) Empirical relations between rock strength and physical properties in sedimentary rocks, *Journal of Petroleum Science and Engineering* 51(3-4): 223-237.
- Cristianini N, Shawe-Taylor J (2000) An introduction to support vector machines and other kernel-based learning methods. Cambridge university press.
- Dehghan AN, Yazdi A (2023) A Geomechanical Investigation for Optimizing the Ultimate Slope Design of Shadan Open Pit Mine, Iran, *Indian Geotechnical Journal*, 1-15.
- Eissa EA, Kazi A (1988) Relation between static and dynamic Young's moduli of rocks, *International Journal of Rock Mechanics and Mining & Geomechanics Abstracts* 25(6):479-482.
- Elkatatny S, Tariq Z, Mahmoud M, Abdulraheem A, Mohamed I (2019) An integrated approach for estimating static Young's modulus using artificial intelligence tools, *Neural Computing and Applications* 31(8):4123-4135.
- Faradonbeh RS, Armaghani DJ, Majid MA, Tahir MM, Murlidhar BR, Monjezi M, Wong HM (2016) Prediction of ground vibration due to quarry blasting based on gene expression programming: a new model for peak particle velocity prediction, *International journal of environmental science and technology* 13(6):1453-64.
- Ferreira C (2001) Gene expression programming: a new adaptive algorithm for solving problems, *Complex Systems* 13(2):87-129.
- Ferreira C (2006) Gene expression programming: mathematical modeling by an artificial intelligence. Springer.
- Fjar E, Holt RM, Raaen AM, Risnes R, Horsrud P (2008) Petroleum related rock mechanics. Elsevier.
- Gholami R, Moradzadeh A, Maleki Sh, Amiri S, Hanachi J (2014) Applications of artificial intelligence methods in prediction of permeability in hydrocarbon reservoirs, *Journal of Petroleum Science and Engineering* 122:643-56.
- Gowida A, Moussa T, Elkatatny S, Ali A (2019) A Hybrid Artificial Intelligence Model to Predict the Elastic Behavior of Sandstone Rocks, *Sustainability* 11(19):5283.

- Jambunathan V (2008) Study of mechanical properties of carbonates. Doctoral dissertation, *University of Oklahoma*.
- James, GA, Wynd, JG (1965) Stratigraphic nomenclature of Iranian oil consortium agreement area. *AAPG bulletin*, 49(12), 2182-2245.
- Jin L, Gupta MM (1999) Stable dynamic backpropagation learning in recurrent neural networks, *IEEE Transactions on Neural Networks* 10(6):1321-1334.
- Karimiazar J, Sharifi Teshnizi E, O'Kelly BC, Sadeghi Sh, Karimizad N, Yazdi A, Arjmandzadeh R (2023) Effect of Nano-Silica on Engineering Properties of Lime-Treated Marl Soil, *Transportation Geotechnics*, 43, 101123.
- Keerthi SS, Lin CJ (2003) Asymptotic behaviors of support vector machines with Gaussian kernel, *Neural computation* 15(7):1667-1689.
- Khaksar A, Taylor PG, Fang Z, Kayes TJ, Salazar A, Rahman K (2009) Rock strength from core and logs, where we stand and ways to go. Conference and Exhibition, European Energy conference.
- King MS (1983) Static and dynamic elastic properties of igneous and metamorphic rocks from the Canadian shield, *Int J Rock Mech Min Sci* 20(5):237-241.
- Knez D, Zamani MAM (2021) Empirical Formula for Dynamic Biot Coefficient of Sandstone Samples from South-West of Poland. *Energies* 14: 5514.
- Lai J, Wang G, Fan Q, Pang X, Li H, Zhao F, Li Y, Zhao X, Zhao Y, Huang Y, Bao M (2022) Geophysical Well-Log Evaluation in the Era of Unconventional Hydrocarbon Resources: A Review on Current Status and Prospects. *Surveys in Geophysics* 43: 913-957.
- Larsen I, Fjaer E, Renlie L (2000) Static and Dynamic Poisson's Ratio of Weak Sandstones. In 4th Rock Mechanics Symposium, North American.
- Mahmoud AA, Elkatatny S, Ali A, Moussa T (2019) Estimation of static young's modulus for sandstone formation using artificial neural networks, *Energies* 12(11):2125.
- Maleki Sh, Gholami R, Rasouli V, Moradzadeh A, Riabi RG, Sadaghzadeh F (2014b) Comparison of different failure criteria in prediction of safe mud weigh window in drilling practice, *Earth-Science Reviews* 136:36-58.
- Maleki Sh, Moradzadeh A, Ghavami R, Sadeghzadeh F (2013) A robust methodology for prediction of DT wireline log, *Iranian Journal of Earth Sciences* 5:33-40.
- Maleki Sh, Moradzadeh A, Riabi RG, Gholami R, Sadeghzadeh F (2014a) Prediction of shear wave velocity using empirical correlations and artificial intelligence methods, *NRIAG Journal of Astronomy and Geophysics* 3(1):70-81.
- Martinez-Ramon M, Christodoulou C (2005) Support vector machines for antenna array processing and electromagnetics, *Synthesis Lectures on Computational Electromagnetics* 1(1):1-20.
- Mitchell M (1996) An introduction to genetic algorithms mit press. Cambridge, Massachusetts, London, England.
- Mostafaei K, Maleki Sh, Mahmoudi MZA, Knez D (2022) Risk management prediction of mining and industrial projects by support vector machine. *Resources Policy* 78: 102819.
- Mostafaei K, Ramazi H (2018) Compiling and verifying 3D models of 2D induced polarization and resistivity data by geostatistical methods, *Acta Geophysica* 66(5):959-971
- Mostafaei K, Ramazi HR (2015) Application of engineering seismic method in calculation of dynamic parameters, case study: Amiriyeh. *New Findings in Applied Geology* 9(18):39-48.
- Plett GL (2003) Adaptive inverse control of linear and nonlinear systems using dynamic neural networks, *IEEE transactions on neural networks* 14(2):360-76.
- Sadooni, F N (1993) Stratigraphic sequence, microfacies, and petroleum prospects of the Yamama Formation, Lower Cretaceous, southern Iraq. *AAPG bulletin*, 77(11), 1971-1988.
- Sanchez AVD (2003) Advanced support vector machines and kernel methods, *Neurocomputing* 55(1-2):5-20.
- Steinwart I, Christmann A (2008) Support vector machines. Springer Science & Business Media.
- Wang HF (2017) Theory of linear poroelasticity with applications to geomechanics and hydrogeology. Princeton University Press.
- Watanabe T, Kasami H, Ohshima S (2007) Compressional and shear wave velocities of serpentinized peridotites up to 200 MPa, *Earth planets and space* 59(4):233-44.
- Zoback MD (2010) Reservoir geomechanics. Cambridge University Press.